Microwire Fibers for Low Loss THz Transmission

Shaghik Atakaramians[a], Shahraam Afshar Vahid[b], Bernd M. Fischer[a],
Heike Ebendorff-Heidepriem[b], Tanya Monro[b] and Derek Abbott[a],

[a]Centre for Biomedical Engineering and School of Electrical & Electronic Engineering,
The University of Adelaide, SA 5005 Australia;
[b]Centre of Expertise in Photonics and School of Chemistry & Physics,
The University of Adelaide, SA 5005 Australia

ABSTRACT

In this paper, we will investigate microwire fibers for low-loss terahertz transmission. Microwires, air-clad wire waveguides with diameter smaller than the operating wavelength (a few μm), have an enhanced evanescent field and tight wave confinement resulting in a low loss waveguide structure for the terahertz (T-ray) frequency regime. Based on our experimental data for the bulk material absorption of four glasses (F2, SF6, SF57 and Bismuth) and a polymer (PMMA), we calculate the normalized field distribution, power fraction outside the wire and effective loss. It will be shown that regardless of material, the effective loss of all microwires converges to the same order < 0.01 cm^{-1}.

Keywords: Terahertz spectroscopy, T-rays, glasses and polymer, microwire, normalized field distribution, power fraction and effective loss

1. INTRODUCTION

The terahertz (THz) or T-ray region of electromagnetic spectrum, located between millimeter wave and infrared frequencies, has attracted much interest over the last decade. Terahertz spectroscopic techniques have many applications in detection of many biological and chemical materials.[1] In almost all terahertz time domain spectroscopy setups free space is being used for propagation of terahertz waves due to the lack of low loss terahertz waveguides. Several waveguide solutions coming from either electronics or photonics have been studied such as the hollow metallic circular waveguide,[2,3] hollow metallic rectangular waveguide,[3] sapphire fiber,[4] plastic ribbon waveguide,[5] air-filled parallel-plate waveguide,[6,7] plastic photonic crystal fiber,[8] coaxial waveguide,[9] metal wire waveguide,[10,11] parallel-plate photonic waveguide,[12] and metal sheet waveguide.[13]

To date, metal parallel plates and bare metal wires are promising metal-based guiding techniques reported in the literature with attenuation constants less than 0.3 cm^{-1} and 0.03 cm^{-1}, respectively.[10,14] Chen et al.[15] have recently reported loss values less than 0.01 cm^{-1} near 0.3 THz in plastic fibers. The concept of THz guided propagation in these fibers is similar to optical nanowire fibers.[16]

Optical nanowires are filaments of dielectric media whose tailorable sub-wavelength dimensions, in the order of nm, allow a substantial fraction of the guided light (wavelength of 1-1.5 μm) to propagate outside the structure. As a result, in this regime, there exists an enhanced evanescent field outside the nanowire.

Further author information:
S.A.: E-mail: shaghik@eleceng.adelaide.edu.au
S.A.: E-mail: shahraam.afsharvahid@adelaide.edu.au
B.F.: E-mail: bfischer@eleceng.adelaide.edu.au
H.E.: E-mail: heike.ebendorff@adelaide.edu.au
T.M.: E-mail: tanya.monro@adelaide.edu.au
D.A.: E-mail: dabbott@eleceng.adelaide.edu.au

Smart Structures, Devices, and Systems III, edited by Said F. Al-Sarawi, Proc. of SPIE
Vol. 6414, 64140I, (2007) · 0277-786X/07/$15 · doi: 10.1117/12.695785

Such an enhanced evanescent field behavior occurs for micrometer diameter fibers in the THz band, whose wavelength ranges from 30 to 3000 μm or equivalently from 0.1 to 10 terahertz. Therefore we coin the term *microwires* for these waveguides used in the terahertz regime.

In this paper, we will describe nanowires and their concept in Section 2. In Section 3 we will describe the terahertz spectroscopy setup and measured optical parameters (absorption coefficient and refractive index) of four glasses (F2, SF6, SF57 and Bismuth) and a polymer (PMMA). In Section 4, by solving the full vectorial Maxwell's equations for a simple rod geometry and using bulk loss coefficients from Section 3, we will demonstrate the normalized field distribution, power fraction and calculated effective loss of microwires made of mentioned glasses and polymer materials.

2. OPTICAL NANOWIRES

In recent years there has been significant interest in metallic or dielectric optical nanowires. The guiding mechanisms of electromagnetic waves in metallic and dielectric nanowires are different. However, in both cases the electromagnetic field is outside the wire. In metallic wires, electromagnetic waves propagate as weakly guided surface waves,[17,18] but in dielectric wires the electromagnetic waves propagate as enhanced evanescent fields. The guiding properties of the modes in metallic wires are modeled under the framework of the Sommerfeld equations, while dielectric wires are analysed calculated by the well known vectorial Maxwell's equations. The diameter of these waveguides are much smaller than the optical wavelength, i.e. in the order of nanometers.

The dielectric nanowire, which is also called an air-clad wire waveguide with subwavelength-diameter core, has interesting properties such as enhanced evanescent fields and tight light confinement—however, its low-loss optical waveguiding is restricted by sidewall smoothness and diameter uniformity, especially when the diameter of the waveguide is very small.[16] In nanowires, coupling between wires can be achieved via surface contact, with extremely small low-loss waveguide curvature, which is an advantage of using such wires.

A question we raise here is: "Is it possible to apply this concept to the terahertz regime?" If yes, under what parameter conditions?

3. BULK MATERIAL LOSS MEASUREMENT

In this section we present the results of loss and refractive index measurements for four glasses (F2, SF6, SF57 and Bismuth) and a polymer (PMMA) in the terahertz (T-ray) regime. To measure the refractive indices and absorption coefficient, we use a commercially available THz time-domain spectrometer (Picometrix T-Ray 2000^{TM}), driven by a Mai-Tai femtosecond laser with a pulse width of less than 100 fs, central frequency of 800 nm and a repetition rate of 80 MHz.[19] The material samples are obtained from the Centre of Expertise in Photonics. The samples are well polished on both sides with cross section of 2 cm $\times$ 2 cm and 0.5 mm thickness. Figure 1(a) shows the prepared samples of SF6, SF57 and Bismuth and Figure 1(b) shows the experimental setup.

The absorption coefficients and refractive indices were obtained by comparing the sample pulses with a reference pulse propagating through dry air. The pulse propagating through the set up when the sample is present is called the sample pulse and when there is no sample it is called the reference pulse. Assuming single mode propagation, the equation for calculating the optical properties can be written in the frequency domain as:

$$\frac{E_{\mathrm{sam}}(\omega)}{E_{\mathrm{ref}}(\omega)} = T_1 T_2 C^2 \exp(-\alpha l/2) \exp(-j\beta_0 (n-1) l) \tag{1}$$

where, $E_{\mathrm{sam}}(\omega)$ and $E_{\mathrm{ref}}(\omega)$ are the complex components at angular frequency ω of the sample and reference electric fields, respectively; T_1 and T_2 are the total transmission coefficients that take into account the reflections at the entrance and exit faces, respectively; C is the coupling coefficient, the same for the entrance and exit faces; β_0 is the free space phase constant; α is the power absorption coefficient; n the refractive index of the sample; and l is the sample length.

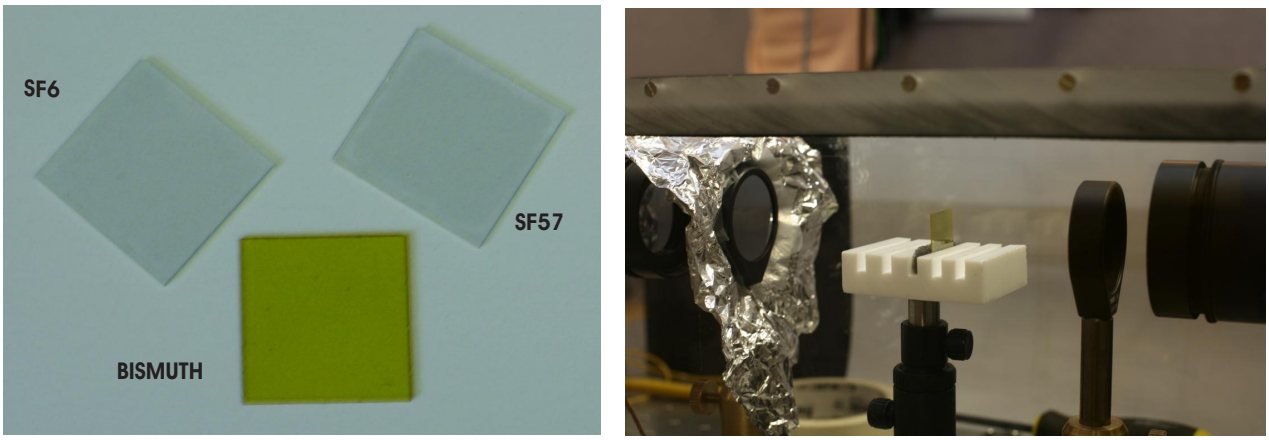

(a) (b)

Figure 1. (a)- Both sides polished: SF6, Bismuth and SF57 samples (b)- Experimental setup and Bismuth sample.

The measured absorption coefficient and refractive indices are shown in Figure 2(a) and Figure 2(b), respectively. The bulk material loss caused by SF6, SF57 and Bismuth were close to each other and were higher than that of F2. Note that PMMA has the lowest material absorption. Individually, the refractive index of each glass sample is significantly higher than the refractive index of the PMMA sample. This results in a tighter confinement of the terahertz radiation in the glass material of a waveguide because of the increased air-glass index change.

It is obvious that if PMMA is used to make conventional waveguides, it will have lower loss in comparison with the other glasses considered here. The question is that what effect do these optical material parameters have on scaled version of nanowires, microwires, in terahertz frequency range?

4. MICROWIRES

The terahertz (T-ray) spectrum has a wavelength range from 30 to 3000 μm. As a result, the enhanced evanescent field phenomenon—observed in optical nanowires with $D << \lambda_{\text{optic}}$—occurs in a dielectric fiber of a few micrometers in diameter, depending on the material used. Thus we use the term "microwire" to describe dielectric fibers with micrometer scale diameter in terahertz frequencies that posses optical nanowire-like properties. In this section, by using the measured optical parameters from Section 3, the normalized electric field distribution, the power fraction outside the fiber, and the effective loss are calculated and discussed.

4.1. Electric field distribution and power fraction

We assume that the wire has a circular cross-section, an infinite air clad, and a step-index profile. It is also assumed that the wire is uniform in diameter and has a smooth sidewall. Considering that the refractive index of air is one and solving the vectorial Maxwell's equation in cylindrical coordinates for the microwire structure; the following eigenvalue equation is achieved for the hybrid modes:[20, 21]

$$\left[\frac{J_n^{'}(u)}{uJ_n(u)}+\frac{K_n^{'}(w)}{wK_n(w)}\right]\left[\frac{J_n^{'}(u)}{uJ_n(u)}+\left(\frac{1}{n_1}\right)^2\frac{K_n^{'}(w)}{wK_n(w)}\right]=n_1^2\left(\frac{1}{u^2}+\frac{1}{w^2}\right)\left[\frac{1}{u^2}+\left(\frac{1}{n_1}\right)^2\frac{1}{w^2}\right] \tag{2}$$

where, J_n is the Bessel function of the first kind, and K_n is the modified Bessel function of the second kind. Here, u and w are normalized transverse wave numbers in the dielectric and air region, respectively; calculated

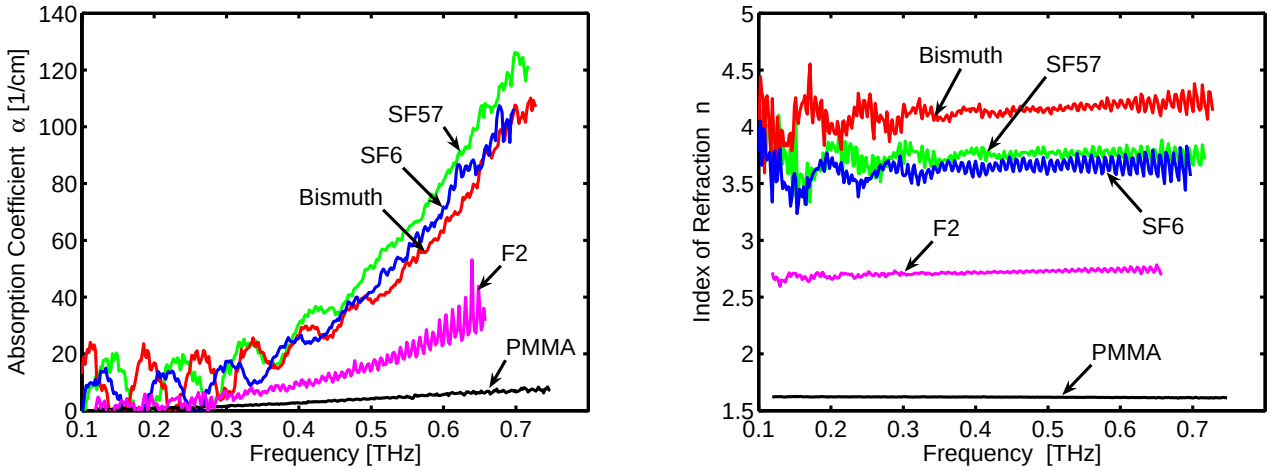

(a) (b)

Figure 2. (a)- Absorption coefficients and (b)- the refractive indices of the bulk materials (PMMA, F2, SF6, SF57 and Bismuth) measured with a THz time domain spectrometer.

as follows:

$$u = a\sqrt{\beta_0^2 n_1^2 - \beta^2} \tag{3}$$

$$w = a\sqrt{\beta^2 - \beta_0^2} \tag{4}$$

where, a is the microwire radius, β_0 is the free space propagating constant, and β is the propagation constant of the hybrid mode that is calculated by solving Equation 2. Having the propagation constant of modes, one can easily calculate the electromagnetic fields in the dielectric (core) and in the air (cladding).[20,21] The normalized electric field component of the fundamental mode in cylindrical coordinates of the air-cladding dielectric wire structure in the microwire regime is depicted in Figure 3(a). The enhanced evanescent field characteristic of the wires made up of glasses (F2, SF6, SF56 and Bismuth) and polymer (PMMA) can be seen for the diameters less than the operating wavelength ($\lambda = 600$ μm, $f = 0.5$ THz).

To obtain more information of the power distribution in the radial direction, the power fraction outside the core is calculated by using the following formula:

$$P_F = \frac{P_{\text{air}}}{P_{\text{total}}} = \frac{\int_a^\infty \int_0^{2\pi} S_{z2} r dr d\phi}{\int_0^a \int_0^{2\pi} S_{z1} r dr d\phi + \int_a^\infty \int_0^{2\pi} S_{z2} r dr d\phi} \tag{5}$$

where, S_{z1} and S_{z2} are the z-component of the Poynting vectors inside and outside the dielectric wire, respectively. Figure 3(b) shows the power fraction outside the wire for the four glasses and the polymer versus the fiber diameter. For the diameters less than the operating wavelength ($\lambda = 600$ μm, $f = 0.5$ THz) the power fraction converges to unity. This can be explained that in this regime, where the diameter is less than the wavelength, most of the guided power is outside the fiber. According to this figure, it can be concluded that the diameter where the fibers enter the microwire operating regime as well as the slope of the convergence of the power fraction strongly depends on the refractive index of the fiber material.

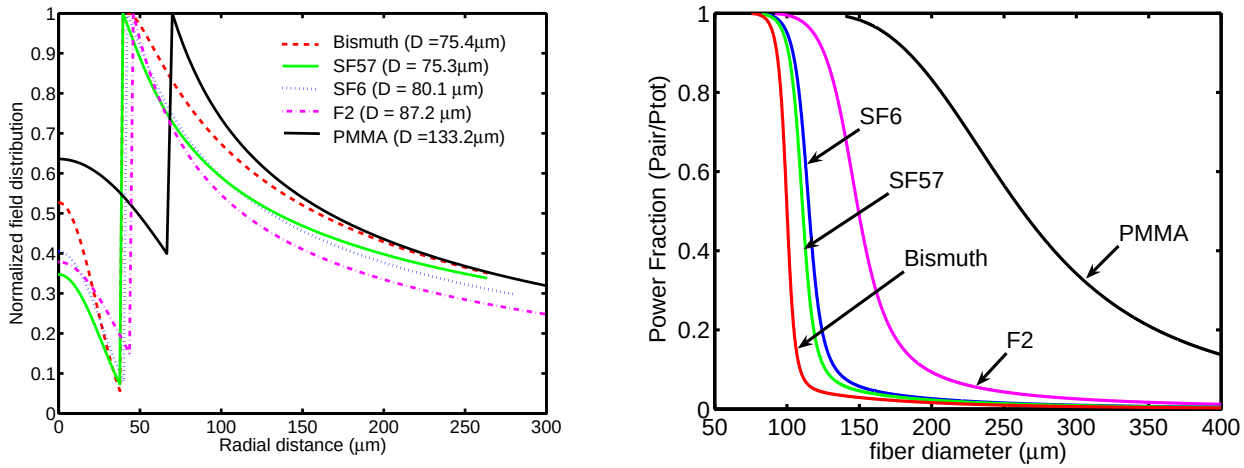

(a) (b)

Figure 3. (a)- Normalized electric field distribution of PMMA, F2, SF6, SF57, and Bismuth microwires versus fiber diameter at $f = 0.5$ THz ($\lambda = 600$ μm) (b)- Power fraction outside the PMMA, F2, SF6, SF57, and Bismuth microwires versus the diameter at $f = 0.5$ THz ($\lambda = 600$ μm).

4.2. Fiber effective loss

An important fiber parameter is the measure of power loss during the transmission of the signals inside the fiber. Fiber losses are due to several effects; among the more important are material absorption, impurity absorption and scattering effects. The material absorption ($\alpha_{\rm m}$) is caused by the molecules of the basic fiber material, either glass or plastic. These losses represent a fundamental minimum to the attainable loss and in conventional fibers can be overcome only by changing the fiber material. In the optical regime, there are materials that have low material absorption. However, the terahertz regime is lacking such materials for proper waveguiding, therefore reducing the fractional power inside the dielectric core—the microwire operating regime—is a way of improving the material absorption[15] .

In the microwire operating regime, the fraction of power outside is more than the fraction of power inside, therefore the material absorption has less effect on the loss. For these wires a new description of material absorption called effective loss—the average of the loss coefficients inside (dielectric) and outside (air) the fiber over the transverse field distributions—is used, which is given by:[22]

$$\alpha_{\rm eff} = \frac{\sigma \int_0^a \int_0^{2\pi} |E|^2 \, r dr d\phi}{\left| \int_0^a \int_0^{2\pi} S_{z1} r dr d\phi + \int_a^\infty \int_0^{2\pi} S_{z2} r dr d\phi \right|} \tag{6}$$

where, σ is the conductivity, related to the material absorption coefficient as follows:[15]

$$\sigma = \frac{n_1 c \alpha_m}{4\pi}, \tag{7}$$

where c the the light velocity in free space.

The calculated effective loss of microwires made up of four glasses and a polymer are shown in Figure 4(a). As expected, the upper limit of the effective loss of different fibers is defined by the bulk material loss. This is where the fiber diameters are at the same order or larger than the THz operating wavelength ($\lambda = 600$ μm),

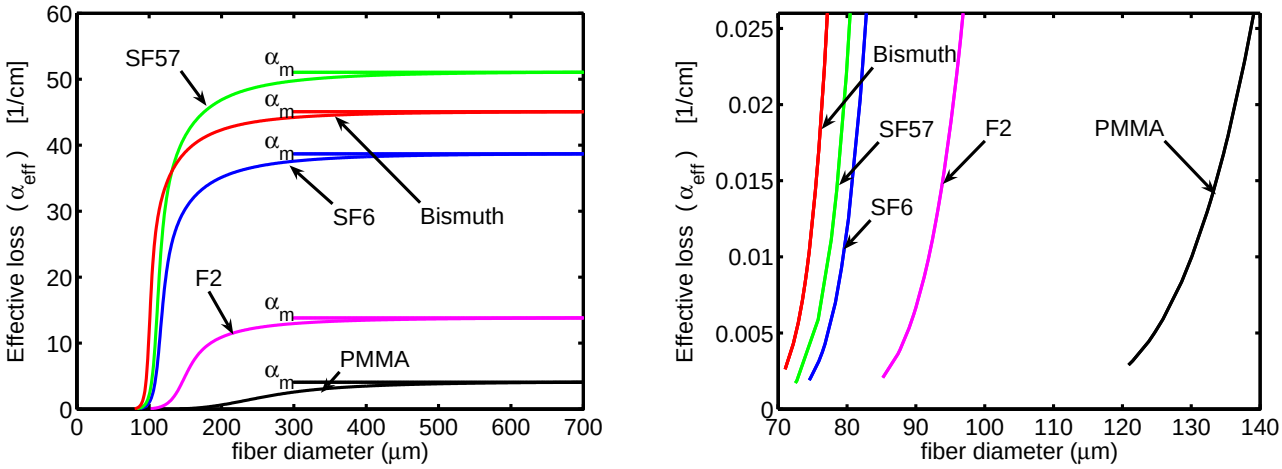

(a) (b)

Figure 4. (a)- Effective loss of fibers made up of PMMA, F2, SF6, SF57 and Bismuth materials versus fiber diameter at $f = 0.5$ THz ($\lambda = 600$ μm) (b)- Magnification of the lower limit of the effective loss shown in Figure 4(a).

therefore the power is confined in the fiber and is encountered with the material loss. For fiber diameters well below the THz operating wavelength (THz microwire operating regime), the effective loss of all five fibers approaches to the same order of value. To have a clear view of this, Figure 4(b) shows the enlargement of effective loss for small diameters, all approaching less than 0.01 cm^{-1} independently of the material. This can be explained by considering that in this regime the field distribution, although guided through the fiber, has the same or a larger amplitude at the dielectric-air interface, resulting in a larger fraction of guided power outside the fiber. It is expected that in this regime, another loss mechanism, i.e. surface roughness scattering, becomes important due to the enhanced evanescent field.

5. CONCLUSION

We use the concept of optical nanowires in the terahertz frequency range to achieve low loss terahertz waveguides. For calculating the normalized field distribution, power fraction outside the waveguide, and fiber effective loss of microwires, we measure the bulk material absorption and refractive index of four glasses (F2, SF6, SF57 and Bismuth) and a polymer (PMMA). We find that in the microwire regime ($D << \lambda_{\mathrm{T-ray}}$) the effective loss of all microwires converges to the same value of loss (less than 0.01 cm^{-1}) regardless of the material used.

Further to the effective loss, nanowires have another loss mechanism due to surface roughness interacting with the enhanced electric evanescent field. It is expected that this limiting factor, loss caused by the surface roughness, will be avoidable for microwires and this is now under investigation.

REFERENCES

1. K. Sakai, *Terahertz Optoelectronics*, Springer, Berlin, Heidelberg, 2005.
2. R. McGowan, G. Gallot, and D. Grischkowsky, "Propagation of ultrawideband short pulses of terahertz radiation through submillimeter-diameter circular waveguides," *Optics Letters* **24**, pp. 1431–1433, 1999.
3. G. Gallot, S. Jamison, R. McGowan, and D. Grischkowsky, "Terahertz waveguides," *Journal of the Optical Society of America B* **17**, pp. 851–863, 2000.

4. S. Jamison, R. McGowan, and D. Grischkowsky, "Singlemode waveguide propagation and reshaping of sub-ps terahertz pulses in sapphire fibers," *Applied Physics Letters* **76**, pp. 1987–1989, 2000.
5. R. Mendis and D. Grischkowsky, "Plastic ribbon THz waveguides," *Journal of Applied Physics* **88**, pp. 4449–4451, 2000.
6. R. Mendis and D. Grischkowsky, "Undistorted guided-wave propagation of subpicosecond terahertz pulses," *Optics Letters* **26**, pp. 846–848, 2001.
7. R. Mendis and D. Grischkowsky, "THz interconnect with low-loss and low-group velocity dispersion," *IEEE Microwave and Wireless Components Letters* **26**, pp. 444–446, 2001.
8. H. Han, H. Park, M. Cho, and J. Kim, "Terahertz pulse propagation in a plastic photonic crystal fiber," *Applied Physics Letters* **80**, pp. 2634–2636, 2002.
9. T.-I. Jeon and D.Grischkowsky, "Direct optoelectronic generation and detection of sub-ps-electrical pulses on sub-mm-coaxial transmission lines," *Applied Physics Letters* **85**, pp. 6092–6094, 2004.
10. K. Wang and D. M. Mittleman, "Metal wires for terahertz wave guiding," *Nature* **432**, pp. 376–379, 2004.
11. T.-I. Jeon, J. Zhang, and D. Grischkowsky, "THz Sommerfeld wave propagation on a single metal wire," *Applied Physics Letters* **86**, 161904, 2005.
12. A. Bingham, Y. Zhao, and D. Grischkowsky, "THz parallel plate photonic waveguide," *Applied Physics Letters* **87**, 051101, 2005.
13. T.-I. Jeon and D. Grischkowsky, "THz Zenneck surface wave (THz surface plasmon) propagation on a metal sheet," *Applied Physics Letters* **88**, 061113, 2006.
14. S. Coleman and D. Grischkowsky, "A THz transverse electromagnetic mode two-dimensional interconnect layer cooperating quasi-optics," *Applied Physics Letters* **83**, pp. 3656–3658, 2003.
15. L.-J. Chen, H.-W. Chen, T.-F. Kao, J.-Y. Lu, and C.-K. Sun, "Low-loss subwavelength plastic fiber for terahertz waveguiding," *Optics Letters* **83**(18), pp. 3656–3658, 2006.
16. L. Tong, R. R. Gattass, J. B. Ashcom, S. He, J. Lou, M. Shen, I. Maxwell, and E. Mazur, "Subwavelength-diameter silica wires for low-loss optical wave guiding," *Nature* **426**, pp. 3656–3658, 2003.
17. A. Sommerfeld, *Electrodynamics*, Academic, New York, 1952.
18. J. Stratton, *Electromagnetic Theory*, McGraw-Hill, New York, 1941.
19. D. Mittleman, *Sensing with Terahertz Radiation*, Springer, Berlin Heidelberg, 2003.
20. A. W. Snyder and J. D. Love, *Optical Waveguide Theory*, Chapman and Hall, London, 1995.
21. K. Okamoto, *Fundamentals of Optical Waveguides*, Academic Press, San Diego, 2000.
22. W. M. Elsasser, "Attenuation in a dielectric circular rod," *Journal of Applied Physics* **20**, pp. 1193–1196, 1949.